Journal of Non-Crystalline Solids 401 (2014) 87–91

Contents lists available at ScienceDirect

Journal of Non-Crystalline Solids

journal homepage: www.elsevier.com/ locate/ jnoncrysol

X-ray absorption spectroscopy of Cu-doped WO_3 films for use in electrochemical metallization cell memory

A. Kuzmin [a,*], A. Anspoks [a], A. Kalinko [a,b], J. Timoshenko [a], R. Kalendarev [a]

[a] Institute of Solid State Physics, University of Latvia, Kengaraga Street 8, LV-1063 Riga, Latvia
[b] Synchrotron SOLEIL, l'Orme des Merisiers, Saint-Aubin, BP 48, 91192 Gif-sur-Yvette, France

ARTICLE INFO

Article history:
Received 29 September 2013
Received in revised form 20 December 2013
Available online 1 February 2014

Keywords:
EXAFS;
XANES;
Thin films;
WO_3;
Electrochemical metallization cell

ABSTRACT

We have performed the first synchrotron radiation X-ray absorption spectroscopy (EXAFS/XANES) study of the local atomic and electronic structure around Cu and W ions in WO_3/Cu/WO_3/Si and WO_3/Cu/Si multilayered structures, aimed for the application in the electrochemical metallization cell memory. The influence of low-temperature annealing at 135 °C has been investigated in details, and a structural model of Cu-doped WO_3 films is proposed.

© 2014 Elsevier B.V. All rights reserved.

1. Introduction

Redox resistive memory (ReRAM) is a promising next-generation memory technology, whose operation is based on the changes of resistance of a metal–insulator–metal structure [1]. It can be realized utilizing electrochemical, thermochemical or valence change phenomena (see [2,3] for details). Only the electrochemical ReRAM type (known also as electrochemical metallization (ECM) cell, conductive bridging cell or programmable metallization cell) will be discussed below. It is based on the electrochemical control of nanoscale quantities of metal in the solid electrolyte thin film, which serves as an active medium [2–5].

An implementation of ECM memory device has been demonstrated on an example of Cu-doped WO_3 films [6–10]. Such device is composed of a thin film of solid WO_3 electrolyte, sandwiched between a copper anode and an inert cathode. One believes that under the influence of electric field, the electron current from the cathode reduces an equivalent number of Cu ions injected from the anode. As a result, a copper metal-rich electrodeposit is formed in the WO_3 electrolyte, and the cell is switched to the low-resistance "ON" state [6–8]. This process can be reversed by applying a bias with opposite polarity, so that the cell returns in the initial high-resistance "OFF" state. Note that the use of SiO_2 [11–13], ZrO_2 [14] and amorphous silicon [15] as solid electrolytes in ECM device has been also successfully tested.

Operating of the ECM cell requires the presence of electrochemically active metal cations within the solid electrolyte matrix, which is usually achieved during the initial electroforming cycle [1,2]. The electroforming process is realized by applying an appropriate voltage pulse, in order to activate bipolar switching behavior. It introduces some amount of metal cations into the thin film acting as electrolyte or promotes the formation of the conductive channel (metallic filament). To reduce the electroforming voltage, some amount of mobile metal ions can be introduced into the electrolyte matrix already during fabrication. The use of the thermal or photo-thermal diffusion processes has been suggested for this purpose in [6,7] to stimulate copper intercalation in Cu-doped WO_3 system. Therefore, the precise knowledge of the local environment around both copper and tungsten ions is of great interest for better understanding of ECM cell functioning. However, this question is a challenging problem.

Previous X-ray diffraction (XRD), Raman spectroscopy and X-ray protoelectron spectroscopy (XPS) studies [6,7] of Cu-doped WO_3 ECM cell gave contradictory results. In [6] no evidence of the formation of Cu-related phases was observed after copper was photodiffused into the amorphous WO_3 film. However, several phases as $CuWO_4$, Cu_2WO_4, Cu_3WO_6, CuO and metallic copper were found in both thermally and photo-thermally diffused films in [7].

In this study we have used direct and non-destructive structural method as synchrotron radiation X-ray absorption spectroscopy to probe the local atomic and electronic structure around copper and tungsten ions in α-WO_3/Cu/α-WO_3/Si and α-WO_3/Cu/Si multilayers both for as-prepared samples and for samples after thermal treatment.

2. Experimental and data analysis

All thin film samples were prepared on unheated silicon substrates using DC magnetron sputtering technique. Layers of amorphous

* Corresponding author.
E-mail address: a.kuzmin@cfi.lu.lv (A. Kuzmin).
URL: http://www.cfi.lv/ (A. Kuzmin).

0022-3093/$ – see front matter © 2014 Elsevier B.V. All rights reserved.
http://dx.doi.org/10.1016/j.jnoncrysol.2014.01.022

tungsten trioxide (α-WO_3) thin film were deposited by sputtering of metallic tungsten target in mixed Ar(80%)–O_2(20%) atmosphere. Layers of metallic copper (Cu) thin film were produced from metallic copper target by sputtering in pure argon atmosphere. The multilayered structures (α-WO_3(250 nm)/Cu(50 nm)/α-WO_3(250 nm)/Si and α-WO_3(500 nm)/Cu(200 nm)/Si) were used as-prepared and after annealing in air at ~135 °C for 30 min to stimulate copper thermal diffusion into tungsten oxide [7]. Pure amorphous α-WO_3 thin film on silicon substrate, metallic copper foil, and polycrystalline CuO powder were also used as references.

The multilayered structures were characterized by micro-Raman spectroscopy (Fig. 1). Raman scattering spectra were collected in back-scattering geometry at 20 °C using a confocal microscope with spectrometer Nanofinder-S (SOLAR TII, Ltd.). Diode-pumped solid-state (DPSS) laser (532 nm, 150 mW cw power) was used as the excitation source, and the Raman scattering spectra were dispersed by 600 grooves/mm diffraction grating mounted in the 520 mm focal length monochromator. The elastic laser light component was eliminated by the edge filter (Semrock LP03-532RE). Peltier-cooled back-thinned CCD camera (ProScan HS-101H, 1024 × 58 pixels) was used as a detector. To avoid possible sample damage, the laser power at the sample was controlled by a variable neutral-density filter (optical density from zero to 3.1).

The Cu K-edge and W L_3-edge X-ray absorption spectra (Fig. 2) were recorded at the C (CEMO) beamline [16] of the HASYLAB/DESY DORIS-III storage ring, operated at $E = 4.44$ GeV and $I_{max} = 140$ mA. The X-ray radiation was monochromatized by a 40% detuned Si(111) double-crystal monochromator. The beam intensity was measured using ionization chambers filled with argon and krypton gases. The 7-cell silicon drift detector (SDD-M3) was used for X-ray fluorescence measurements. X-ray absorption spectra of the multilayered structures were recorded in the fluorescence mode, whereas all other samples were measured in the transmission mode.

The extended X-ray absorption fine structure (EXAFS) spectra $\chi(k)$ were extracted and analyzed following the conventional procedure [17] using the EDA software package [18]. Particular attention has been paid to the accurate alignment of the experimental and theoretical (calculated by the FEFF8 code [19]) scales in the k-space by fine tuning of the E_0 parameter in the definition of the photoelectron wavenumber $k = \sqrt{\left(2m_e/\hbar^2\right)(E-E_0)}$, where m_e is the electron mass, $\hbar$ is the Plank constant and E is the X-ray photon energy [17]. The first coordination shell of tungsten atoms and the first two coordination shells of copper atoms were isolated using the Fourier filtering procedure and best-fitted within the single-scattering Gaussian approximation [18].

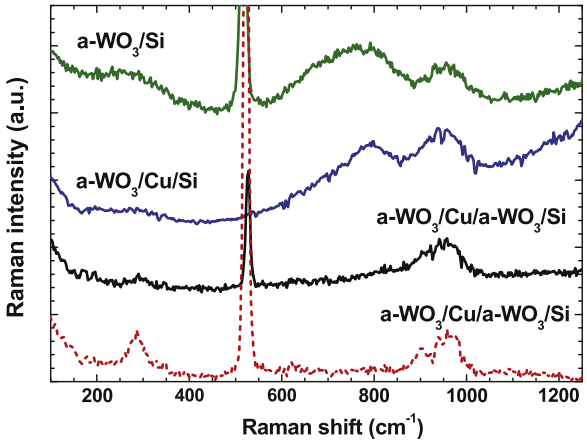

Fig. 1. Raman scattering spectra for α-WO_3/Si, α-WO_3/Cu/Si and α-WO_3/Cu/α-WO_3/Si samples. The lowest Raman spectrum (dashed curve) has been measured using the full laser power.

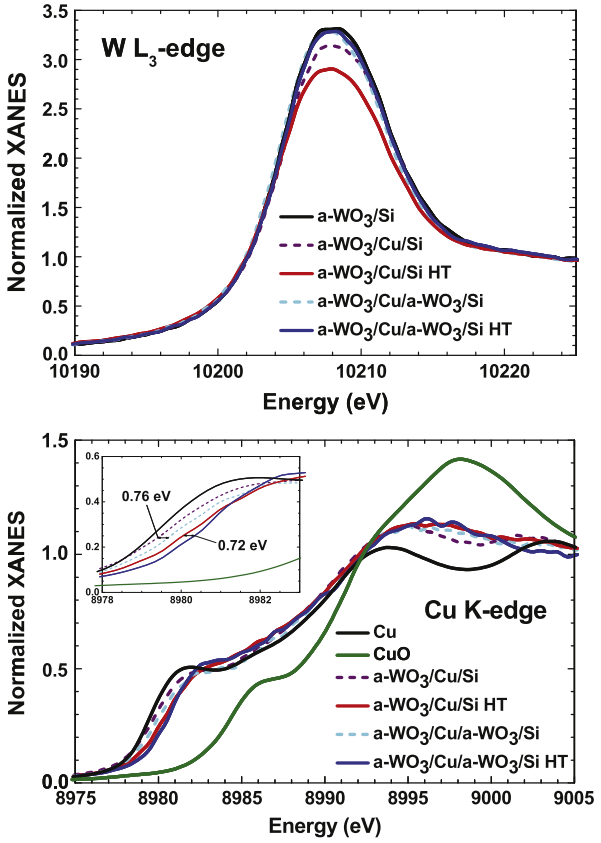

Fig. 2. Normalized W L_3-edge and Cu K-edge XANES spectra, recorded at 300 K in α-WO_3/Cu/α-WO_3/Si and α-WO_3/Cu/Si multilayers before and after high-temperature (HT) annealing at 135 °C. The experimental data for α-WO_3/Si thin film, metallic Cu and CuO are also shown for comparison.

The theoretical backscattering amplitude and phase shift functions for W–O, Cu–O and Cu–Cu atom pairs were calculated using the ab initio real-space FEFF8 code [19,20]. The FEFF8 calculations were first performed for several reference compounds ($CuWO_4$ [21], Cu_2O [22], CuO [23] and metallic copper [24]) based on their crystallographic structures. The complex exchange-correlation Hedin–Lundqvist potential was used in the FEFF8 calculations to account for the inelastic losses [20]. The amplitude and phase shift functions calculated for Cu_2O [22] were finally used in the analysis of the Cu K-edge EXAFS spectra for the multilayered structures.

3. Results

The Raman spectra of α-WO_3/Si film and α-WO_3/Cu/Si multilayer are dominated by two bands, located at 750 cm^{-1} and 950 cm^{-1} (Fig. 1). These two bands are commonly assigned to the stretching modes of the bridging O – W – O and terminal W═O bonds, respectively [25,26]. Note that the band due to terminal W═O bonds is the strongest in α-WO_3/Cu/α-WO_3/Si multilayer. The weaker band at 250–300 cm^{-1} is observed in all three samples and is attributed to the bending O – W – O modes [25,26]. The Raman band at 520 cm^{-1} is due to silicon substrate [27]: it is not visible in α-WO_3/Cu/Si sample due to sufficiently thick copper layer. No crystalline phases due to copper and tungsten oxides have been observed in our samples.

We would like to note that by increasing the laser power above some threshold a local crystallization of the multilayers can be induced (see dashed curve in Fig. 1). As a result, two new bands appear at 286 cm^{-1} and 900 cm^{-1} due to CuO and $CuWO_4$ phases, respectively. Also the second-order Raman scattering from silicon substrate becomes visible at 960 cm^{-1}, indicating enhanced transparency of the film.

Normalized W L_3-edge and Cu K-edge X-ray absorption near-edge structure (XANES) spectra, recorded at $T = 300$ K, are shown in Fig. 2 for α-WO_3/Cu/α-WO_3/Si and α-WO_3/Cu/Si multilayers before and after high-temperature (HT) annealing at 135 °C, as well as for several reference materials (metallic Cu, CuO powder and amorphous α-WO_3/Si thin film). Note that no edge shift is observed between the W L_3-edge XANES spectra for multilayers and α-WO_3/Si thin film. However, the energy position of the shoulder at the Cu K-edge in multilayers is closer to that in metallic copper than in CuO (see inset in Fig. 2), and it also shifts by 0.72–0.76 eV upon annealing.

The FTs of the W L_3-edge EXAFS spectra (Fig. 3) are dominated by the first coordination shell (peak at 1.3 Å), composed of oxygen atoms, followed by the multiple-scattering contribution from the first shell (peaks at 2–3 Å) and the second coordination shell (peak at 3–4 Å), composed mainly of tungsten atoms [28,29]. The similarity of Fourier transforms (FTs) for the W L_3-edge in the as-prepared and annealed multilayered structures to that for pure α-WO_3 thin film indicates that the local environment around tungsten atoms is close in all samples and is weakly influenced by the presence of copper atoms (Fig. 3). This fact is in agreement with high crystallization temperature (above 400 °C [27]) of pure amorphous tungsten trioxide films.

At the same time, the local environment of copper atoms depends strongly on the type of the multilayered structure and annealing procedure (Fig. 3). There are two main types of nearest neighbors (oxygen and copper) bonded to copper atoms. Therefore, the Cu – O bonds are responsible for the peak at 1.4–1.6 Å, whereas the Cu – Cu bonds give the origin of the peak at 2.25 Å. The analysis of the outer coordination shells around copper is a significant challenge and is beyond the scope of the present study.

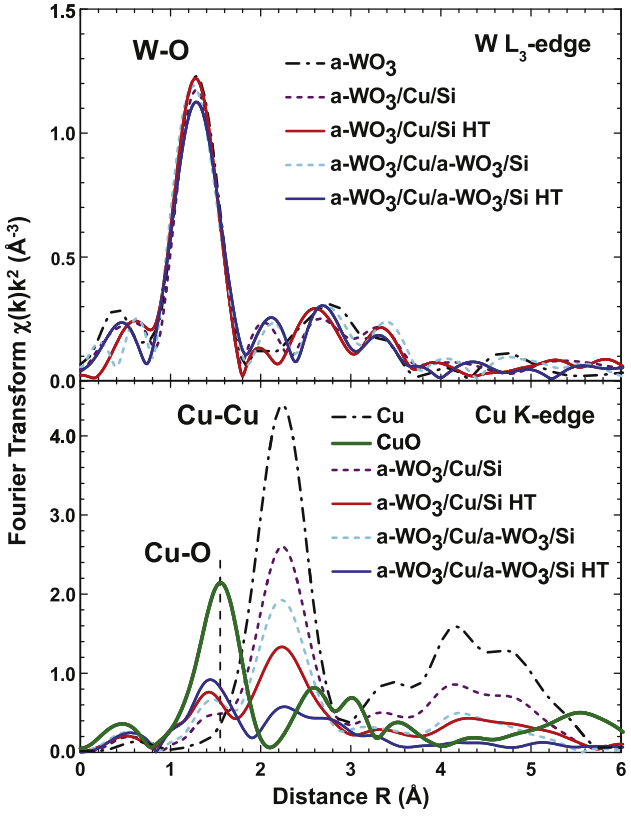

Fig. 3. Fourier transforms (FTs) of the W L_3-edge and Cu K-edge EXAFS spectra $\chi(k)k^2$, recorded at $T = 300$ K, in α-WO_3/Cu/α-WO_3/Si and α-WO_3/Cu/Si multilayers before and after high-temperature (HT) annealing at 135 °C. The experimental data for metallic Cu, CuO and amorphous α-WO_3/Si thin film are also shown for comparison. Note that the peaks in FTs do not appear at the true interatomic distances due to the extra phase shifts [17].

The experimental Cu K-edge EXAFS spectra in the multilayers before and after high-temperature (HT) annealing at 135 °C are shown in Fig. 4 (left panel). Before annealing they are dominated by a contribution of metallic copper, which diminishes upon annealing. In the right panel of Fig. 4 we show an example of the best-fit results for the first coordination shell (the range of ~0.8–2.4 Å for the W L_3-edge and ~0.8–2.0 Å for the Cu K-edge in Fig. 3) of tungsten and copper in α-WO_3/Si thin film, CuO powder and annealed α-WO_3/Cu/α-WO_3/Si multilayer.

As a result of the fit, a set of structural parameters (coordination numbers N, interatomic distances R and mean-square relative displacements (MSRDs) σ^2) has been obtained. We found that tungsten atoms have strongly distorted octahedral coordination, which is close in all samples. There are four nearest oxygen atoms at R(W–O) ≈ 1.80 ± 0.02 Å with σ^2(W–O) ≈ 0.011 ± 0.003 Å and two distant oxygen atoms at R(W–O) ≈ 2.13 ± 0.03 Å with σ^2(W–O) ≈ 0.004 ± 0.002 Å. Note that static disorder gives main contribution into the MSRDs σ^2(W–O).

The local environment of copper atoms is less distorted. In CuO powder, copper atoms are four-fold coordinated by oxygens located at R(Cu–O) ≈ 1.940 ± 0.004 Å with σ^2(Cu–O) ≈ 0.0033 ± 0.0007 Å^2. At the same time, the average Cu – O bond length in the multilayers is significantly shorter. We found that after high-temperature (HT) annealing at 135 °C copper atoms, located in the tungsten oxide matrix, are two-fold coordinated by oxygens located at R(Cu–O) ≈ 1.88 ± 0.01 Å with σ^2(Cu–O) ≈ 0.005 ± 0.001 Å^2. Note that the decrease of copper coordination number from 4 to 2 oxygen atoms correlates well with the shortening of the average Cu–O distance by ~0.06 Å.

4. Discussion

The W L_3-edge XANES (Fig. 2) is dominated by the intense peak at 10,207 eV, a so-called "white line" (WL), which is due to the dipole-allowed transition ($\Delta l = +1$, l is the orbital momentum) 2p(W)→$\overline{5,\epsilon}$d (W). Here the bar over $\overline{5,\epsilon}$ indicates that the final state of the electron in the continuum (ϵ) with 5d(W) atomic character is the relaxed excited state in the presence of the core-hole at the 2p(W) level screened by other electrons [28,29]. Due to the large value of the absorption coefficient, the WL amplitude cannot be usually determined accurately, however the WL shape and energy position are very close in all our compounds. This result indicates that the local electronic structure of

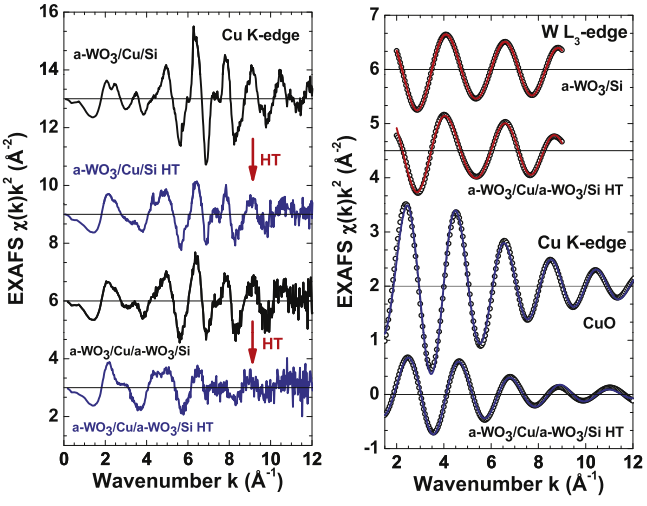

Fig. 4. Left panel: experimental Cu K-edge EXAFS spectra $\chi(k)k^2$ in the multilayers before and after high-temperature (HT) annealing at 135 °C. Right panel: Comparison of the experimental (open circles) and best-fit (solid lines) first shell W L_3-edge and Cu K-edge EXAFS spectra $\chi(k)k^2$ for the W – O and Cu – O bonds in α-WO_3/Si, CuO and α-WO_3/Cu/α-WO_3/Si multilayer after high-temperature (HT) annealing at 135 °C. The EXAFS signals in both panels are shifted vertically for clarity.

tungsten atoms remains also close. Taking also into account the similarity of Fourier transforms (FTs) for the W L_3-edge, one can conclude that introducing copper ions into α-WO_3 matrix produces negligible effect on the host matrix structure. Therefore, we will further concentrate our attention on the local environment of copper atoms.

The Cu K-edge XANES spectra for multilayers and two reference compounds, shown in Fig. 2, indicate that there is a clear difference in the effective charge of copper ions. Our XANES spectra for metallic copper and CuO agree with known data in [30–32] and show a well defined shoulder at the onset of the absorption edge, which is due to the dipole-allowed transition $1s(Cu) \rightarrow \overline{4,\epsilon}p(Cu)$ [30]. The energy positions of the shoulder for our as-prepared multilayers, defined at the maximum of the first derivative, are at 8979.4 eV for α-WO_3/Cu/Si and 8979.7 eV for α-WO_3/Cu/α-WO_3/Si: both values are slightly larger than that (8979.2 eV) for metallic Cu. Upon thermal treatment of multilayers at 135 °C, the shoulder position shifts to larger energies by about 0.72–0.76 eV, becoming close to that in Cu_2O [31]. Thus, the analysis of the Cu K-edge XANES suggests that copper ions are present mainly as Cu^0 in the as-prepared samples, but transfer into Cu^+ upon annealing.

This result is fully confirmed by the analysis of EXAFS data, shown in Fig. 3. In the as-prepared samples, copper is mostly present in the metallic phase characterized by the strong peak at 2.25 Å in the FTs of the Cu K-edge EXAFS: it corresponds to the true distance Cu–Cu of about 2.56 Å. Also the outer peaks at 3–6 Å in the FTs have a shape similar to that in metallic copper. The amplitude of the FT peaks suggests the presence of strong disorder and size reduction effect in the as-prepared α-WO_3/Cu/Si and α-WO_3/Cu/α-WO_3/Si films. Closer inspection of the FTs shows that some small part of copper atoms is oxidized already in the as-prepared samples, as is evidenced by the presence of the peak at 1.43 Å, which is due to a contribution of oxygen atoms located in the first coordination shell of copper.

The annealing of the multilayered structures at 135 °C provokes further oxidation and diffusion of copper. While metallic copper is still present in α-WO_3/Cu/Si after annealing, it disappears completely in α-WO_3/Cu/α-WO_3/Si sample. In both cases, the intensity of the peak at 1.43 Å due to the bonds Cu – O increases. A detailed analysis (Fig. 4 (right panel)) indicates that the copper coordination in the multilayers is equal to about two oxygen atoms located at the distance of ~1.88 Å. Such coordination of copper ions is close to that observed for Cu^+ in Cu_2O ($N = 2$, $R = 1.85$ Å) [22]. For comparison, copper coordination of four oxygen atoms at ~1.94 Å was found by us in CuO (Fig. 4 (right panel)), in agreement with crystallographic data [23]. Thus, the oxidation of copper ions in the multilayers upon annealing determined from the Cu K-edge EXAFS spectra confirms the results of XANES analysis discussed before.

The obtained information on the behavior of copper ions in α-WO_3 solid electrolyte matrix allows us to propose the schematic model of α-WO_3/Cu/Si and α-WO_3/Cu/α-WO_3/Si multilayered structures. Upon annealing at 135 °C a part of copper atoms, forming the bottom electrode, diffuses into α-WO_3 matrix in the first case (Fig. 5(a)), whereas metallic copper layer becomes fully dissolved in the solid electrolyte in the second case (Fig. 5(b)). Our results suggest that different technological approaches can be used to introduce mobile metal ions into the electrolyte matrix during fabrication to simplify the electroforming process [1,2].

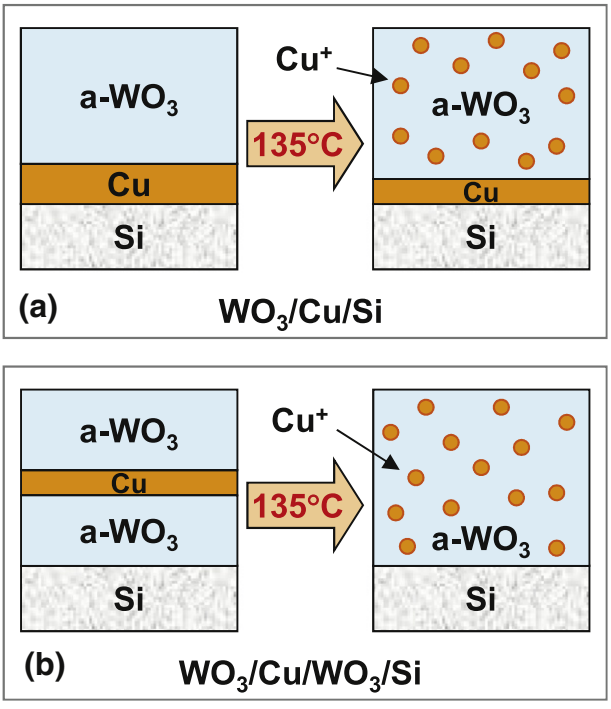

Fig. 5. Schematic models for (a) α-WO_3/Cu/Si and (b) α-WO_3/Cu/α-WO_3/Si multilayers before and after high-temperature (HT) annealing at 135 °C.

5. Conclusions

X-ray absorption spectroscopy at the W L_3 and Cu K edges was employed to study the local atomic and electronic structure of α-WO_3/Cu/Si and α-WO_3/Cu/α-WO_3/Si multilayered structures, which are developed for the application in the electrochemical metallization cell (ECM) memory.

We have shown that the as-prepared multilayers contain nanosized metallic copper, which is oxidized to Cu^+ upon annealing at ~135 °C. The monovalent copper ions have small ion size and, thus, are able to diffuse across the multilayer and participate in the formation of conducting pathways in the ECM cell during its operation [1–3]. No copper containing crystalline phases have been found in the present study opposite to the previous work [7].

Acknowledgments

This work was supported by the Latvian National Research Program IMIS and the European Social Fund within the project 2009/0138/1DP/1.1.2.1.2/09/IPIA/VIAA/004 (Support for Doctoral Studies at the University of Latvia). The EXAFS experiments at HASYLAB/DESY were supported by the EC FP7 under grant agreement No. 226716. We would like to thank Dr. R. Chernikov for assistance during the experiment at the beamline.

References

[1] R. Waser, M. Aono, Nat. Mater. 6 (2007) 833.
[2] R. Waser, R. Dittmann, G. Staikov, K. Szot, Adv. Mater. 21 (2009) 2632.
[3] I. Valov, R. Waser, J.R. Jameson, M.N. Kozicki, Nanotechnology 22 (2011) 254003.
[4] M.N. Kozicki, M. Park, M. Mitkova, IEEE Trans. Nanotechnol. 4 (2005) 331.
[5] W. Lu, D.S. Jeong, M. Kozicki, R. Waser, MRS Bull. 37 (2012) 124.
[6] M.N. Kozicki, C. Gopalan, M. Balakrishnan, M. Mitkova, IEEE Trans. Nanotechnol. 5 (2006) 535.
[7] C. Gopalan, M.N. Kozicki, S. Bhagat, S.C.P. Thermadam, T.L. Alford, M. Mitkova, J. Non-Cryst. Solids 353 (2007) 1844.
[8] Y. Li, S. Long, Q. Liu, Q. Wang, M. Zhang, H. Lv, L. Shao, Y. Wang, S. Zhang, Q. Zuo, S. Liu, M. Liu, Phys. Status Solidi (RRL) 4 (2010) 124.
[9] L. Ying-Tao, L. Shi-Bing, L. Hang-Bing, L. Qi, W. Qin, W. Yan, Z. Sen, L. Wen-Tai, L. Su, L. Ming, Chin. Phys. B 20 (2011) 017305.
[10] C. Kügeler, R. Rosezin, E. Linn, R. Bruchhaus, R. Waser, Appl. Phys. A 102 (2011) 791.
[11] C. Schindler, S.C.P. Thermadam, R. Waser, M.N. Kozicki, IEEE Trans. Electron Devices 54 (2007) 2762.
[12] S.P. Thermadam, S.K. Bhagat, T.L. Alford, Y. Sakaguchi, M.N. Kozicki, M. Mitkova, Thin Solid Films 518 (2010) 3293.
[13] S.C. Puthentheradam, D.K. Schroder, M.N. Kozicki, Appl. Phys. A 102 (2011) 817.
[14] Q. Liu, C. Dou, Y. Wang, S. Long, W. Wang, M. Liu, M. Zhang, J. Chen, Appl. Phys. Lett. 95 (2009) 023501.
[15] Y. Yang, P. Gao, S. Gaba, T. Chang, X. Pan, W. Lu, Nat. Commun. 3 (2012) 732.
[16] K. Rickers, W. Drube, H. Schulte-Schrepping, E. Welter, U. Bruggmann, M. Herrmann, J. Heuer, H. Schulz-Ritter, AIP Conf. Proc. 882 (2007) 905.
[17] V.L. Aksenov, A.Yu. Kuzmin, J. Purans, S.I. Tyutyunnikov, Phys. Part. Nucl. 32 (2001) 675.

[18] A. Kuzmin, Physica B 208–209 (1995) 175.
[19] A.L. Ankudinov, B. Ravel, J.J. Rehr, S.D. Conradson, Phys. Rev. B 58 (1998) 7565.
[20] J.J. Rehr, R.C. Albers, Rev. Mod. Phys. 72 (2000) 621.
[21] A. Kuzmin, A. Kalinko, R.A. Evarestov, Acta Mater. 61 (2013) 371.
[22] M. Dapiaggi, W. Tiano, G. Artioli, A. Sanson, P. Fornasini, Nucl. Instrum. Methods Phys. Res. B 200 (2003) 231.
[23] H. Yamada, X.-G. Zheng, Y. Soejima, M. Kawaminami, Phys. Rev. B 69 (2004) 104104.
[24] M.E. Straumanis, L.S. Yu, Acta Crystallogr. A 25 (1969) 676.
[25] J.V. Gabrusenoks, P.D. Cikmach, A.R. Lusis, J.J. Kleperis, G.M. Ramans, Solid State Ionics 14 (1984) 25.
[26] M.F. Daniel, B. Desbat, J.C. Lassegues, B. Gerand, M. Figlarz, J. Solid State Chem. 67 (1987) 235.
[27] A. Kuzmin, R. Kalendarev, A. Kursitis, J. Purans, J. Non-Cryst. Solids 353 (2007) 1840.
[28] A. Kuzmin, J. Purans, J. Phys. Condens. Matter 5 (1993) 2333.
[29] A. Kuzmin, J. Purans, J. Phys. Condens. Matter 5 (1993) 9423.
[30] S. Bocharov, Th. Kirchner, G. Dräger, O. Šipr, A. Šimůnek, Phys. Rev. B 63 (2001) 045104.
[31] J.Y. Kim, J.A. Rodriguez, J.C. Hanson, A.I. Frenkel, P.L. Lee, J. Am. Chem. Soc. 125 (2003) 10684.
[32] J. Chaboy, A. Muñoz-Páez, E. Sánchez Marcos, J. Synchrotron Radiat. 13 (2006) 471.